# **Ibuprofen Loaded Sodium Alginate Sponges for Acute Wound Treatment**

Kadir AYKAÇ\*°, Ceyda KÖROĞLU ÖZMEN\*\*

Ibuprofen Loaded Sodium Alginate Sponges for Acute Wound Treatment

Yara Tedavisi İçin İbuprofen Yüklü Sodyum Aljinat Süngerler

#### **SUMMARY**

In this study, the potential of ibuprofen-loaded sodium alginate sponges for wound treatment was investigated through in vitro and cell culture cytotoxicity assays. Sodium alginate solutions at two different concentrations were dried using a lyophilizer to obtain drug delivery systems in the form of sponges containing various concentrations of ibuprofen. The prepared formulations were characterized for critical properties including water-holding capacity, molecular interactions (FTIR), tissue elasticity (texture analysis), drug content, drug release kinetics, and cytotoxicity. The results showed that the sponges could absorb water up to 5 times their own weight and dissolved completely within 2 hours, with a faster drug release observed compared to pure ibuprofen. Drug release kinetics revealed that Formulation A followed a first-order kinetic model, while Formulation B conformed to the Hopfenberg model. Cytotoxicity tests indicated that pure ibuprofen exhibits dosedependent toxicity, however this was significantly reduced when incorporated into the sodium alginate formulation. Overall, the findings suggest that ibuprofen-loaded sodium alginate sponges have a high potential for use in wound treatment.

Keywords: Ibuprofen, sponges, wound treatment.

## ÖZ

Bu çalışmada, ibuprofen yüklü sodyum aljinat süngerlerinin yara tedavisinde kullanım potansiyeli in vitro ve hücre kültürü-sitotoksisite çalışmaları ile araştırılmıştır. Bu amaçla, iki farklı derişimde hazırlanan sodyum aljinat çözeltileri, liyofilizatör aracılığıyla kurutularak, çeşitli derişimlerde ibuprofen içeren sünger formunda ilaç taşıyıcı sistemler elde edilmiştir. Hazırlanan formülasyonların su tutma kapasitesi, moleküler etkileşimleri (FTIR), doku esnekliği (tekstür analizleri), etkin madde miktarı, ilaç salım kinetiği ve sitotoksisitesi gibi kritik özellikleri incelenmiştir. Çalışma sonucunda, süngerlerin kendi ağırlığının 5 katına kadar su tutabildiği ve 2 saat içinde tamamen çözündüğü gözlenmiştir. Ayrıca, saf ibuprofene kıyasla etkin madde salımının daha hızlı olduğu tespit edilmiştir. İlaç salım kinetiği incelendiğinde, A formülasyonlarının birinci derece kinetik modele, B formülasyonlarının ise Hopfenberg modeline uyduğu belirlenmiştir. Sitotoksisite testleri, saf ibuprofenin doza bağlı toksisite gösterdiğini, ancak sodyum aljinat formülasyonuna katılmasıyla bu toksisitenin azaldığını ortaya koymuştur. Elde edilen bulgular, ibuprofen yüklü sodyum aljinat süngerlerin yara tedavisinde kullanım potansiyelinin yüksek olduğunu göstermektedir.

Anahtar Kelimeler: İbuprofen, sünger, yara tedavisi.

Recieved: 15.09.2025 Revised: 10.10.2025 Accepted: 15.10.2025

ORCID: 0000-0001-7426-1332, Department of Pharmaceutical Technology, Faculty of Pharmacy, Anadolu University, Eskişchir, Türkiye.

<sup>&</sup>quot;ORCID: 0000-0001-5326-7495, Department of Pharmaceutical Biotechnology, Faculty of Pharmacy, Anadolu University, Eskişehir, Türkiye.

## INTRODUCTION

Dermal injuries are wounds on the skin, often caused by cuts, incisions, or bruises. Wound healing outcomes are significantly influenced by numerous factors, including tissue perfusion, oxygen saturation, infectious agents, edema, local inflammation, systemic stress, metabolic status, nutritional deficiencies, and coexisting morbidities (Tottoli et al., 2020). Wound healing is a complex physiological process that restores skin integrity and regenerates damaged tissues, involving various cell populations, the extracellular matrix, and soluble mediators such as growth factors and cytokines (Velnar et al., 2009). The wound healing process occurs in four consecutive yet overlapping phases. This progression involves hemostasis for cessation of hemorrhage, inflammation for the recruitment of necessary immune cells, proliferation for new tissue synthesis, and re-epithelialization to ultimately restore the functional skin barrier (Guo & DiPietro, 2010; Peña & Martin, 2024). Due to its vital role as a barrier, cutaneous wound healing is an indispensable survival mechanism that facilitates to wound closure and tissue restoration. The process is physiologically complex, relying on the coordinated action of diverse cell populations and molecular mediators. These elements engage in an intricate, temporally sequenced cascade to ensure the structural and functional re-establishment of the dermis (Pazyar et al., 2014; Sorg et al., 2017).

The inflammatory phase, which succeeds the initial injury, encompasses both hemostasis and cutaneous neurogenic inflammation (Schultz et al., 2011). The inflammatory phase, which begins immediately after injury and lasts around an hour, is marked by blood clotting and the activation of the innate immune system, thereby setting the stage for healing. A rapid influx of neutrophils then occurs within 24 hours to eliminate pathogens and clear the wound. These cells gradually decrease over the next week as the healing process moves forward (Cañedo-Dorantes & Cañedo-Ayala, 2019). Hemostasis is initially

established through the formation of a platelet plug, subsequently stabilized by the development of a fibrin matrix that provides a provisional scaffold for cellular infiltration and tissue regeneration (Yang et al., 2021). The proliferative phase begins 2-10 days after injury, focusing on new tissue formation. This involves cell proliferation and migration, leading to the formation of highly vascularized granulation tissue in the dermis. Simultaneously, re-epithelialization begins as keratinocytes migrate from the wound edges to restore the skin's structural and functional integrity (Tottoli et al., 2020).

Non-steroidal anti-inflammatory drugs (NSAIDs) are used to manage tissue injury by providing analgesic, anti-inflammatory, and antipyretic effects which improve patient comfort and recovery (Chen & Dragoo, 2013). While the long-term use of NSAIDs for chronic wounds is debated due to concerns that they may impair healing, a growing body of evidence supports their beneficial short-term use. Administering of NSAIDs for a brief period can reduce excessive inflammation, enhance patient comfort, and foster a more favorable environment for wound healing to progress (Anderson & Hamm, 2012). Ibuprofen (2-(4-isobutylphenyl)propanoic acid) is a widely used NSAID, employed to treat a variety of conditions, including fever, pain, and inflammation. In wound healing, ibuprofen's ability to modulate inflammation provides both symptomatic relief and regulation of the tissue repair process. The analgesic and anti-inflammatory effects of ibuprofen arise from the inhibition of Cyclooxygenase (COX) enzymes, thereby reducing prostanoid synthesis and mitigating pain and inflammation (Rainsford, 2009). While the application of NSAIDs for wound healing is a contentious issue, studies on formulations containing ibuprofen are frequently reported in the literature. Furthermore, ibuprofen has been utilized within the context of wound healing, where its capacity to modulate inflammation contributes not only to symptomatic relief but also to the regulation of the tissue repair process (Anderson

& Hamm, 2012; Andrgie et al., 2020a; Jan-Roblero & Cruz-Maya, 2023; Khalil et al., 2025; Morgado et al., 2017; Price et al., 2007).

Over the past decades, a diverse range of advanced wound dressing materials (e.g., microneedles, hydrocolloids, hydrogels, nanofibers, foams, and films) has been investigated, with the collective purpose of optimizing the wound healing microenvironment by regulating moisture balance, reducing microbial invasion, and providing the structural scaffolding necessary for tissue regeneration (Long et al., 2022; Sadeghi-Aghbash et al., 2023; Tenorová et al., 2022; Wang et al., 2022). Sponges are effective wound dressings primarily due to their porosity, high absorption capacity, and air permeability, properties that allow them to promote rapid hemostasis. 3D porous structure of sponges also allows them to act as carriers for bioactive agents (like anti-inflammatory or antibacterial substances), which enhances their therapeutic potential in wound healing (Long et al., 2022).

Alginates are linear, water-soluble, and highly swellable anionic polysaccharides naturally derived from the cell walls of brown algae (Shaikh et al., 2022). Alginate biopolymers are composed of 1,4-linked β-D-mannuronic acid (M) and α-L-guluronic acid (G) monomers, which are arranged in block-like sequences that can be either heterogeneous (MG) or homogeneous (poly-M, poly-G). Owing to their inherent hydrophilic properties, alginates can be processed into sponge-like forms, making them suitable for application on wounds, where they promote moisture retention and facilitate the healing cascade (Barbu et al., 2021). A study reported the development of ibuprofen-loaded nanofibers. The resulting controlled-release system demonstrated sustained drug release that extended for 14 days (Mohiti-Asli et al., 2017). In another study, thermosensitive hydrogel systems were developed, and nearly 70% ibuprofen release was observed after 3 days (Andrgie et al., 2020b). Alginates are well known for accelerating the healing of wounds in humans. After lyophilization, which creates the porous structure, the resulting sponge is used as a topical application matrix (Dai et al., 2009). Sodium alginate has become a preferred material for wound dressings due to its biocompatibility, low immunogenicity, water retention and degradability (Lv et al., 2022). Also, it is highly hydrophilic, enabling it to absorb wound exudate, maintaining a moist microenvironment. Combined with its biodegradability and antibacterial activity, sodium alginate's utilization in creating a 3D porous, high-swelling sponge is a highly promising strategy for managing wounds and burns (Hu et al., 2018; Naghshineh et al., 2019). Most studies focused on wound healing are directed toward controlled and sustained release (Djekic et al., 2020; Romanelli et al., 2009). While many studies focus on controlled and long-term drug delivery, the release of ibuprofen was conversely aimed to be accelerated and its relative solubility enhanced in this study. To achieve this, ibuprofen-loaded, water-soluble sodium alginate sponges were developed, and lyophilization was utilized in their fabrication to ensure a porous and stable structure.

### MATERIALS AND METHODS

#### **Materials**

Ibuprofen was kindly gifted from Drogsan, Turkey. Sodium alginate was purchased from Sigma Aldrich, Germany. Acetonitrile was provided Carlo Erba, Italy. All other chemicals used were in analytical grade.

# Preparation of sponges

Sodium alginate solutions were prepared at 2% and 5% (w/w) concentrations by dissolving the polymer in distilled water based on prior studies with modifications (Wang et al., 2023). To these solutions, different ratios of ibuprofen in ethanol (as detailed in Table 1.) were added and mixed on a magnetic stirrer for 10 minutes to ensure homogeneity. The resulting formulations were then frozen at -20 °C and subsequently lyophilized to produce porous sponges. Freeze-drying process facilitated the removal of water by sublimation, which is crucial for creating the desired spongy structure.

Table 1.	Composition	of sponges
----------	-------------	------------

Formulation	Sodium alginate (mg)	Sodium alginate (mg) Distilled water (g) Ibuprofen (mg)		Ethanol (mL)
A0	500	25	-	1
A1	500	25	165	1
A2	500	25	330	1
ВО	1250	25	-	1
B1	1250	25	165	1
B2	1250	25	330	1

Ibuprofen is a chemically stable drug with a typical shelf life of at least two years under standard storage conditions (Farmer et al., 2002). Consequently, preservative-free solution formulations of ibuprofen are available on the market (Üstünes, 2025). In the preparation of ibuprofen sponges, stability testing was omitted from the scope of the study because the manufacturing process does not involve exposure to temperature and heat that threaten stability, and because the formulations prepared via lyophilization result in a solid matrix form.

## **HPLC** conditions

A method was used to determine the amount of ibuprofen in drug content and release studies using High-Performance Liquid Chromatography (HPLC). The analysis was performed on a C18 column (250 x 4.6 mm, 5 µm), with a mobile phase consisting of acetonitrile, distilled water, and o-phosphoric acid (70:30:1). A photodiode array detector was set to a wavelength of 225 nm. The system operated at a flow rate of 1 mL/min, and the injection volume was 20 µL (Namazov, 2022) chronic or acute pain, as well as as an antipyretic in both children and adults. The negative effects of NSAIDs on the duodenum and stomach in the gastrointestinal tract (GIS). The HPLC method was validated for the study, considering linearity, precision, accuracy, selectivity, and stability parameters. The linear equation was obtained as y = 37579x +10380 (r<sup>2</sup>=0.9999).

# Water absorption capacity and porosity tests

100 mg sponges were weighed then placed in 10 mL phosphate buffer solution (PBS). After 5 minutes

sponges were weighed again. The percentage of the amount of water absorbed to the sponge weight was determined (n=3) (Petchsomrit et al., 2017).

Porosity was determined using the ethanol displacement method. An initial ethanol volume  $(V_1)$  was measured (n=3). A certain sponge sample was immersed, and the resulting volume  $(V_2)$  was recorded. After 5 minutes, the sample was removed, the final ethanol volume  $(V_3)$  was measured, and porosity was calculated from these volumes according to equation (1) (Naghshineh et al., 2019):

$$\frac{V_1 - V_3}{V_2 - V_3} \times 100 \tag{1}$$

## Fourier transform infrared analyses

To determine the structural properties, Fourier transform infrared spectroscopy (FTIR; IRAffinity-1S Shimadzu, Japan) was performed. The analyses were conducted in the 4000 to 500 cm<sup>-1</sup> range with a high-sensitivity DLATGS detector and a Germanium-coated KBr beam splitter. The spectra of pure ibuprofen and sodium alginate were used as reference materials for comparison.

## Morphological analyses

The morphology and porosity of the sponges were determined using Scanning Electron Microscopy (SEM). Analysis was conducted on a Carl Zeiss SU-PRA 50VP SEM (Oberkochen, Germany) at a constant voltage of 15 kV, various magnifications, and a temperature of 25±2 °C.

## **Texture analyses**

The mechanical strength of the sponges was assessed using a texture analyser (TA.XT plus, Stable

Micro Systems, UK). Compression mode was chosen to evaluate the flexibility of the sponges. For analyses, the force required for the probe to advance 4 mm into the sponges was measured (n=3).

## Drug content and loading capacity

The amount of ibuprofen in the sponges was determined using HPLC. A sponge sample (5 mg) was initially dissolved in 10 mL of a 1:1(v/v) mixture of ethanol and distilled water. The resulting solution was then filtered (0.45  $\mu$ m) before being analyzed by the HPLC system. In pharmaceutical analyses, the drug content is determined by calculating the proportion of the active drug component within the formulation and expressing this as a percentage. To calculate the drug loading capacity, the drug content is divided by the total amount of ibuprofen used, and the result is expressed as a percentage (Khoukhi et al., 2016).

## In vitro drug release and release kinetics

In vitro drug release studies were conducted using the dialysis bag method (Yurtdaş-Kırımlıoğlu et al., 2018). Drug release was evaluated using sponge samples loaded with 2 mg of ibuprofen. Furthermore, to achieve sink conditions, the study was completed using a sponge formulation containing one-fifth of the saturated concentration of ibuprofen. The experiment was conducted in a 50 mL release medium of pH 7.4 PBS, with the temperature strictly maintained at 37±1 °C to simulate physiological conditions (Mohandas et al., 2015)we have developed a bi-layered sponge that promotes fibrin clot stability and prevents secondary bacterial wound infections. Using the technique of freeze-drying, a bi-layer matrix consisting of hyaluronic acid (HA. To assess the in vitro release profile, samples were withdrawn from the release medium at predetermined time points (0.5, 1, 1.5, 2, 3, 4, 5, and 7 hours). An equal volume of fresh medium was simultaneously replaced (Stoyanova et al., 2016)characterized by dissolution-limited oral bioavailability. One approach to improve its water solubility and bioavailability is by solubilizing it in micellar surfactant solutions. Here we investigate the effect of the surfactant type and the mechanism of solubility enhancement of Ibuprofen in surfactant solutions. The equilibrium Ibuprofen solubility in solutions of six surfactants was determined by HPLC. The nonionic surfactant polysorbate 80 (Tween 80). The amount of ibuprofen in each sample was quantified via HPLC (n=3). The data was analyzed using DDSolver to model the drug release kinetics (Zhang et al., 2010).

# Cytotoxicity study

The cytotoxicity of the drug formulations was evaluated using the MTT assay on human umbilical vein endothelial cells (HUVEC) (Romani et al., 2024). This protocol was adapted from a similar MTT assay previously described (Yalçınkaya et al., 2025). HUVEC cells were maintained in Dulbecco's Modified Eagle Medium (DMEM) supplemented with 10% fetal bovine serum (FBS) and 1% penicillin-streptomycin. For the assay, cells were seeded into 96-well plates at a density of 2×10<sup>4</sup> cells and incubated for 24 hours at 37 °C in a humidified atmosphere with 5% CO2. After the initial incubation, cells were treated with various concentrations of the formulations and ibuprofen (20-300 µg/mL). The formulation and active substance were dissolved in fresh medium. All procedures were carried out aseptically in a Laminar Flow Cabinet (Kojair, Finland). Following 24 and 48 hours of treatment, the medium was removed and 20 μL of MTT solution (5 mg/mL in PBS) was added to each well. The plates were then incubated for another 3 hours to allow formazan crystal formation. Subsequently, the MTT solution was carefully removed, and 200 µL of dimethyl sulfoxide (DMSO) was added to dissolve the resulting formazan crystals. The absorbance was measured at 570 nm using a microplate reader (Cytation 5, BioTek, UK), and the resulting values were used to calculate cell viability. Viability was expressed as a percentage relative to the untreated control cells, which were considered to have 100% viability. All experiments were conducted in triplicate.

#### RESULTS AND DISCUSSION

## Preparation of sponges

During preparation, Formula B's sodium alginate solutions were more viscous. The addition of ibuprofen made the solutions opaque, as the drug precipitated due to its insolubility in the alginate solutions (Garzón & Martínez, 2004). To ensure a homogeneous distribution of ibuprofen within the sponge, the solutions were stirred on a magnetic stirrer at 750 rpm for 30 minutes before being placed in the refrigerator. After lyophilization, the porous morphology of the sponges was visually apparent. Organoleptic controls revealed that the sponges from Formula A exhibited a softer and more flexible texture, which was attributed to their lower sodium alginate content.

## Water absorption capacity and porosity test

Table 2 presents the water absorption capacity and porosity results. The sodium alginate sponges demon-

strated the ability to absorb 2.9 to 5 times their weight in water within a mere 5-minute period. Despite the higher sodium alginate content in Formula B delaying the process, the high hydrophilicity of all sponges led to rapid dissolution and a loss of structural stability within 1-2 hours. To improve structural integrity, sodium alginate is commonly cross-linked with calcium ions. However, the ions present in PBS can disrupt this structure by interacting with the calcium (Chiaoprakobkij et al., 2011). In Formula A, an increase in ibuprofen content led to a decrease in water absorption capacity due to a higher ibuprofen-to-sodium alginate ratio. Conversely, no direct relationship was found between this ratio and water retention in Formula B. Porosity analysis indicated that the formulations exhibited varying degrees of porosity. However, no direct correlation was established between the ibuprofen concentration and the resulting porosity. The results confirmed the porous nature of the sponges.

<b>Table 2.</b> Results of water absorption capacity and porosity tests (n=3; mean
--

Code	Absorption of Water %	Porosity %		
A0	358.1978±62.0942	75.07±7.77		
A1	328.3034±29.3729	38.07±3.77		
A2	291.8699±31.4725	73,24±1.29		
В0	449.4580±75.5654	59.10±3.97		
B1	460.0879±25.8998	64.20±1.72		
B2	500.5849±67.9352	60.40±2.82		

# Fourier transform infrared analyses

FTIR spectroscopy is a powerful, high-resolution technique that measures the vibrational frequencies of chemical bonds to identify functional groups and characterize chemical structures, including surface components and drug-polymer interactions (Liu et al., 2018). FTIR analysis results are shown in Figure 1. The FTIR spectrum of ibuprofen reveals its molecular structure through several characteristic absorption bands. A strong band at 2953 cm<sup>-1</sup> is assigned to the CH<sub>3</sub> asymmetric stretching vibration, while a very strong peak at 1712 cm<sup>-1</sup> is a clear indicator of the C=O stretching motion. Aromatic C=C bonds are

observed in the region of 1460–1550 cm<sup>-1</sup> and a band at 1417 cm<sup>-1</sup> is attributed to the C–C stretching vibration in aromatic ring. Additionally, a very strong peak at 1230 cm<sup>-1</sup> for C-C stretching and a strong band at 779 cm<sup>-1</sup> for CH<sub>2</sub> vibrations serve as the molecule's unique fingerprint. Other observed features include CH<sub>3</sub> rocking (strong intensity) at 935 cm<sup>-1</sup> and CH<sub>2</sub> asymmetric stretching at 2920 cm<sup>-1</sup>. The medium intensity O-H...O valence stretching vibrations at 2727 cm<sup>-1</sup> and 2630 cm<sup>-1</sup> confirm the presence of a hydrogen-bonded dimer. In addition, various in-plane and out-of-plane C-H and O-H deformations were noted at multiple frequencies, with all assigned bands align-

ing with the known functional groups of ibuprofen (Kamari & Ghiaci, 2016; Namazi et al., 2019; Ramukutty & Ramachandran, 2012).

The carboxylate anion form (COO-) is observed at 1597 cm<sup>-1</sup>. The band at 821 cm<sup>-1</sup> is characteristic of mannuronic acid residues within the sodium alginate structure. The bands at 1076 cm<sup>-1</sup> and 1024 cm<sup>-1</sup> are assigned to the C-O and C-C stretching vibrations

of the pyranose ring, as well as the C-O-C glycosidic bonds. The band at 1297 cm<sup>-1</sup> is assigned to skeletal vibration. Additionally, the band at 1406 cm<sup>-1</sup> is attributed to the C-OH deformation vibration and the symmetric O-C-O stretching vibration of the carboxylate group. Finally, a weak signal around 2956 cm<sup>-1</sup> is due to C-H stretching vibrations (Huang et al., 2017; Lawrie et al., 2007).

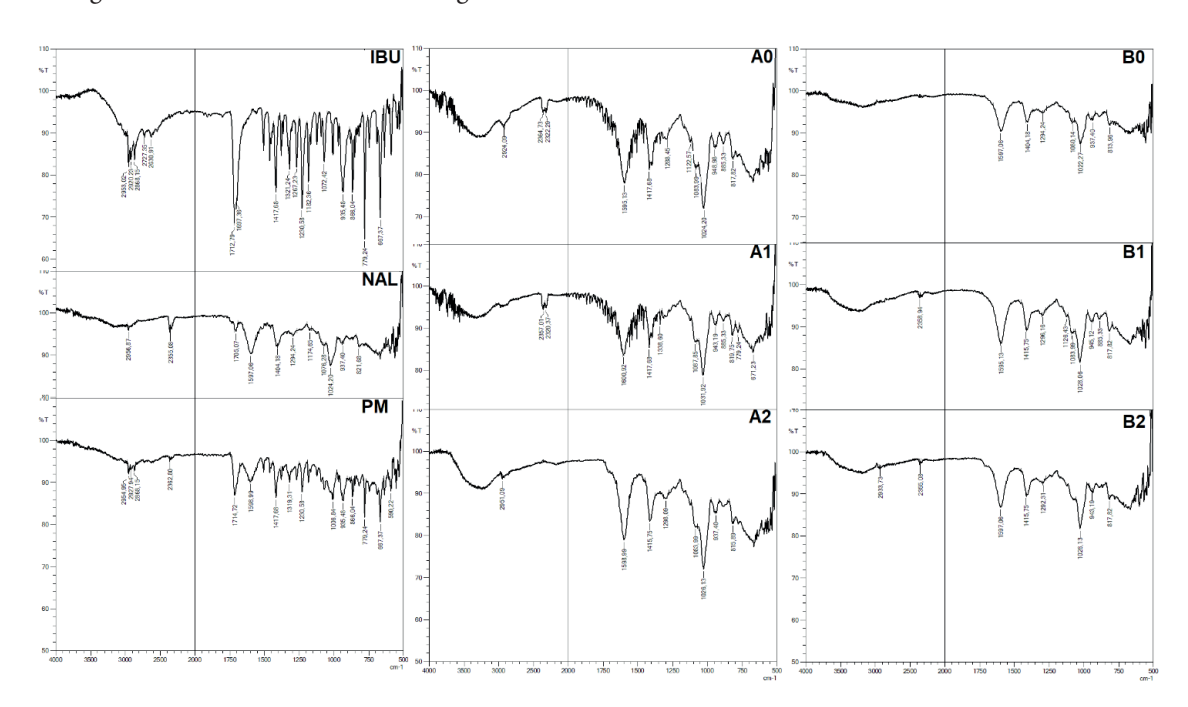


**Figure 1.** FTIR results of formulations; IBU: Ibuprofen, NAL: Sodium Alginate, PM: Physical mixture of sodium alginate and ibuprofen

Characteristic bands for sodium alginate were detected in both A0 and B0 formulations, with minor shifts in the peaks at 817, 1024, 1083, 1288, 1597, and 2364 cm<sup>-1</sup>. The FTIR spectrum of the physical mixture revealed characteristic peaks of both ibuprofen and sodium alginate. The prominent bands at 2954, 1714, 1417, 1319, 1230, 935, 866, 779, and 667 cm<sup>-1</sup> are attributed to ibuprofen, while the peak at 1598 cm<sup>-1</sup> is assigned to the carboxylate anion of sodium alginate. Analysis of the A1 spectrum revealed distinct peaks corresponding to both ibuprofen and sodium alginate. Specifically, ibuprofen is represented by peaks at 671, 779, and 1417 cm<sup>-1</sup>, while characteristic sodium alginate peaks appear at 1031, 1087, 2357, and 1600 cm<sup>-1</sup>.

The spectrum further showed a lack of peaks at 2727 and 2630 cm<sup>-1</sup>, which implies the absence of hydrogen bonding within the A1 formula (Kumar et al., 2014; Ramukutty & Ramachandran, 2012).

The FTIR spectrum of the A2 formula exhibits characteristic peaks for sodium alginate at 937, 1026, 1083, and 1598 cm<sup>-1</sup>, and a peak for ibuprofen at 1415 cm<sup>-1</sup>. A significant finding is the disappearance of the characteristic ibuprofen peaks that were present in the physical mixture spectrum, which was observed in both A1 and A2 formulations. This spectral change is likely caused by the electrostatic interaction between sodium alginate and ibuprofen (Liu et al., 2019) including the zein final concentration, the mass ratio of

zein to SC, and the mass ratio of SC to SA influence the physicochemical properties of the nanoparticles. The fluorescence spectrum confirmed that curcumin was encapsulated in the composite nanoparticles with an increase in the mass ratio of curcumin to zein, and the encapsulation efficiency of curcumin decreased. When coated with SA, there was a significantly improved encapsulation efficiency. Fourier transform infrared spectroscopy (FTIR). The FTIR spectrum of the B1 formula showed that only the ibuprofen peak at 1415 cm<sup>-1</sup> (C-C stretching vibration in aromatic ring) remained. Furthermore, slight displacements were noted in the peaks assigned to sodium alginate. This trend is also replicated in the B2 formula. The FTIR results show that ibuprofen maintains its stability in sodium alginate sponges.

## Morphological analyses

SEM images (Figure 2.) confirmed the porous structure of the sponges. Pores were observed to be irregularly distributed throughout the sponge matrix. Formula B, prepared with a higher sodium alginate percentage, exhibited distinct porosity compared to Formula A.

## **Texture analysis**

The texture analysis results are presented in Figure 3. Formula B0, requires a force of 50 N to be compressed by 4 mm, whereas for A0, this force is 6 N. The sponge texture becomes increasingly soft as the concentration of ibuprofen rises in the B formulations. Approximately 15 N is required to compress Formula B1 by 4 mm, while this value is 10 N for Formula B2. Conversely, Formula A1 was determined to have the softest sponge texture. For Formula A2, the required force increased significantly as the distance increased. This suggests that the sponge is nearing its incompressibility point. In a study conducted by Boateng et al., sodium alginate wafers were prepared at five different concentrations (1% to 5%), utilizing paracetamol as a model drug. According to the texture analysis data obtained from the study, the maximum force required to compress a 2% concentration wafer by 2 mm was recorded as 20.6 N, while this value was observed to be 93.7 N for the 5% concentration. In comparison, it was determined that the ibuprofen-loaded sponge formulations possessed a softer texture, despite being subjected to similar preparation processes (Boateng et al., 2010).

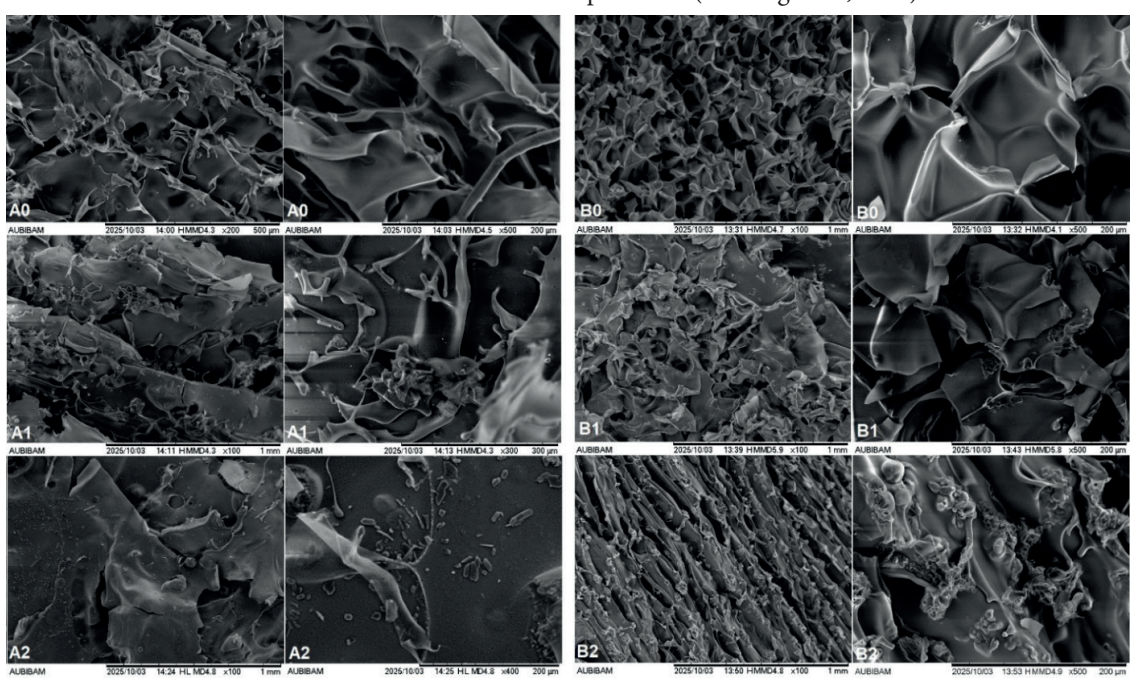
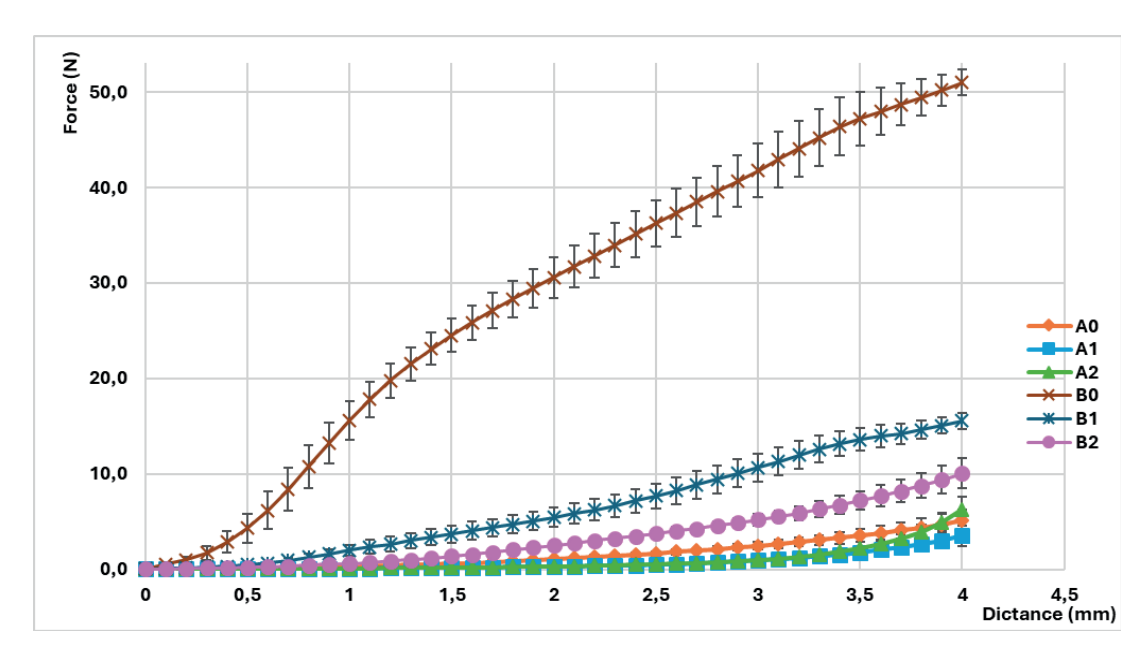


Figure 2. SEM imaging results of formulations



**Figure 3.** Texture analysis result of sponges (n=3, mean  $\pm$  SE)

# Drug content and loading capacity

The amount of ibuprofen in the sponges is given in Table 3. Formula B1 demonstrated the highest loading capacity, closely followed by B2, while formula A1 exhibited the lowest. This loss of active substance occurred during the formulation preparation, specifically high-vacuum drying process (Li & Yang, 2015). Furthermore,3 the inherent hygroscopicity of sodium alginate led to a mass increase, caused by the entrapment of distilled water during the preparation of the solution, which consequently reduced the loading capacity (Xie et al., 2022; Zhang et al., 2024).

**Table 3.** Drug content of sponges (n=3; mean  $\pm$  SE)

Formulation	Drug Content (% w/w)	Loading Capacity (w/w)	
A1	$10.31 \pm 0.43$	41.56 ± 1.73	
A2	24.85 ± 0.84	62.56 ± 2.11	
B1	$9.40 \pm 0.80$	80.58 ± 3.96	
B2	15.21 ± 1.23	72.93 ± 5.91	

## In vitro drug release and release kinetics

Based on data from *in vitro* release studies, formula B2 was identified as the fastest-releasing formulation. Conversely, formula A2, while being the slowest-releasing formulation, still achieved about 100% release

within 4 hours (Figure 4.). The prepared formulations enhanced the dissolution rate of ibuprofen (Kaynak et al., 2024). This is particularly notable given that ibuprofen's solubility is pH-dependent, with studies consistently demonstrating an increase in solubility as the pH rises (Higton, 2015; Janus et al., 2020). The pH of sodium alginate solutions typically ranges from 8 to 10 (Latifah et al., 2022). Micro-environmental pH changes and physical interactions with the sodium alginate matrix accelerate ibuprofen solubility (Arica et al., 2005). Immediate release of ibuprofen was also observed in another study that utilized cross-linked sodium alginate beads (Li et al., 2021). In addition to ibuprofen's high solubility in basic environments due to its acidic nature (pKa: 5.2), the polymer/dissolution medium coefficient is also a significant factor influencing the dissolution rate. The inclusion of sodium alginate has been shown to increase the ibuprofen release rate. This is attributed to the excipient's ability to generate osmotic forces capable of disrupting the membranous barrier, which facilitates a higher rate of drug release (Majid Khan & Bi Zhu, 1998). These findings align with and confirm the release results observed in our study.

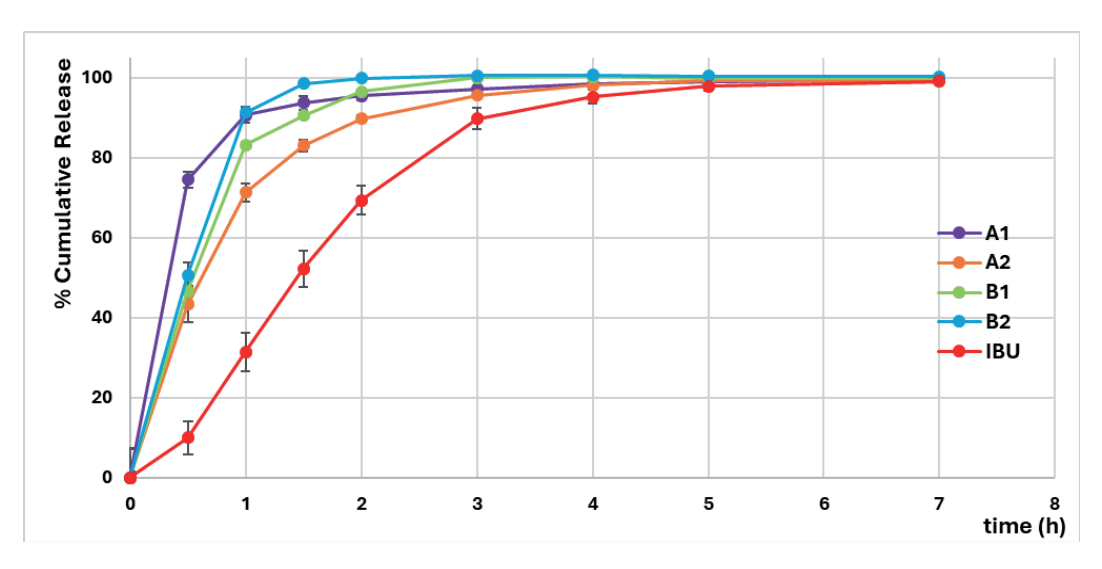


**Figure 4.** *In vitro* drug release results (n=3, mean  $\pm SE$ )

The prepared sponge formulations conformed to different release kinetics, as shown in Table 4. The data were analyzed using DDSolver (Zhang et al., 2010). The lowest Akaike Information Criterion (AIC), highest Model Selection Criterion (MSC), and coefficient of determination (r²<sub>adj</sub>) values were used to select the appropriate kinetic model (Zuo et al., 2014). The release kinetics of formulations A1 and A2 were first-order, while the Hopfenberg model was suitable for B1 and B2. In contrast, pure ibuprofen conformed to the Hixson-Crowell model.

Under first-order release kinetics, the drug release rate is directly proportional to the amount of drug remaining in the matrix. Consequently, as the drug concentration decreases, the release rate slows down proportionally. This principle is consistent with the Noyes-Whitney equation (Dokoumetzidis & Macheras, 2006). Consequently, this model is particularly well-suited for porous matrices that contain water-soluble components, where the dissolution and diffusion processes are the primary factors controlling the drug release profile (Askarizadeh et al., 2023).

The Hopfenberg model describes drug release from surface-eroding polymers with a constant surface area. In this model, matrix erosion and time are the limiting factors, influenced by internal and external diffusional resistance (Gupta et al., 2020). This model is relevant for surface-eroding polymers, where the drug release rate is directly influenced by the rate of polymer matrix degradation from the surface (Paarakh et al., 2018). The Hopfenberg model, which assumes matrix erosion is the rate-limiting step for drug release, was a good fit for cylindrical (n=2) and spherical (n=3) systems, respectively, as it accounts for the formulation's geometry (Vidart et al., 2018). For the B1 formula, which exhibited Hopfenberg kinetics, the release exponent (n value) was found to be 4.125. In contrast, the B2 formula showed an n value of 3, consistent with release from a spherical structure (Katzhendler et al., 1997). Drug transport and release from pharmaceutical systems is a complex process driven by a combination of physical and chemical phenomena, making it challenging to develop an accurate mathematical model (Costa & Sousa Lobo, 2001).

**Table 4.** Kinetic models of formulations

		Release Models					
Code	Parameters	Zero Order	First Order	Higuchi	Korsmeyer-Peppas	Hixon-Crowell	Hopfenberg
A1	k	21.940	2.380	51.780	86.312	0.250	0.250
	r <sub>2ad</sub> j	-39.414	0.872	-11.870	0.733	-9.576	-6.827
	AIC	80.927	34.894	71.772	41.533	70.202	68.561
	MSC	-3.949	1.805	-2.805	0.975	-2.609	-2.403
	n	-	-	-	0.096	-	3.000
	k	21.307	1.114	49.075	65.312	0.237	0.277
	r <sup>2</sup>	-3.582	0.991	-0.008	0.725	0.483	0.804
A2	AIC	77.218	27.342	65.103	55.475	59.765	52.753
	MSC	-1.772	4.462	-0.258	0.946	0.410	1.286
	n	-	-	-	0.290	-	5.250
	k	21.931	1.750	51.055	71.270	0.249	0.311
	r <sup>2</sup> adj	-5.523	0.940	-0.736	0.557	-0.193	0.980
B1	AIC	79.161	41.590	68.570	58.410	65.568	33.759
	MSC	-2.125	2.571	-0.802	0.469	-0.426	3.550
	n	-	-	-	0.240	-	4.125
	k	22.285	3.075	52.284	39.042	0.240	0.480
	r <sup>2</sup> adj	-7.632	0.622	-1.577	-4.322	-0.613	0.966
B2	AIC	80.443	55.414	70.774	77.340	67.026	36.812
	MSC	-2.406	0.723	-1.197	-2.018	-0.728	3.048
	n	-	-	-	0.503	-	3.000
	k	19.597	0.528	42.823	42.356	0.135	0.135
	r <sup>2</sup> adj	0.467	0.940	0.855	0.735	0.961	0.954
IBU	AIC	68.890	51.380	58.486	64.082	48.029	50.029
	MSC	0.380	2.569	1.680	0.981	2.987	2.737
	n	-	-	-	0.423	-	3.000

An analysis of the models suggests that the drug release mechanism in the B formulations involves a combination of swelling, matrix erosion, and mixed diffusion and chain relaxation mechanisms. Considering the porous structure of the sponges and the water solubility of sodium alginate, the release kinetics of formulations A1 and A2 were found to be first-order, which is a result consistent with the literature. The elevated sodium alginate concentration in Formula B, as opposed to Formula A, led to a modification of the release kinetics. This difference is characterized by ibuprofen release being primarily driven by the structural erosion of the sponge matrix. While the precise mechanism for the release of ibuprofen from the B1

formulation has not been elucidated in the existing literature, evidence suggests that the process proceeds via super-case II transport (Martín-Illana et al., 2022).

The difference factor  $(f_1)$  and similarity factor  $(f_2)$  are key metrics for assessing the difference and similarity between two drug release profiles. An f1 value of 0–15 and an  $f_2$  value of at least 50 are the established criteria for similarity, as per EMA and FDA guidelines. Both factors are widely used to compare the release rates of drug delivery systems (Muselík et al., 2021; Priese et al., 2023) neither the EMA nor the FDA provides unambiguous instructions for comparing the dissolution curves, except for calculating the similarity factor f2. In agreement with the EMA and FDA

strategy for comparing the dissolution profiles, this manuscript provides an overview of suitable statistical methods (CI derivation for f2 based on bootstrap, CI derivation for the difference between reference and test samples, Mahalanobis distance, model-dependent approach and maximum deviation method. The prepared sponge formulations, in this case, have different release profiles than pure ibuprofen, as shown by the results (Table 5.) obtained in this study.

**Table 5.** Similarity and difference factors of formulations versus pure ibuprofen

Formulation	(f <sub>1</sub> ) Difference factor	(f <sub>2</sub> ) Similarity factor	
A1	037	022	
A2	025	032	
B1	032	027	
B2	036	024	

## Cytotoxicity study

Due to its biocompatibility and ability to support tissue regeneration, alginate is a favorable polymer for wound healing applications (da Silva et al., 2024). The cytotoxicity of the formulations was evaluated using an MTT assay on human umbilical vein endothelial cells (HUVECs), with the results presented in Figure 5 (Jiang et al., 2021). Additionally, cell cultures in the

multi-well plates were routinely monitored via microscopy throughout the study, and no evidence of contamination was observed.

Based on the MTT assay results, the empty formulation containing 5% alginate exhibited a higher proliferative effect, leading to significantly higher cell viability compared to the 2% alginate empty formulation. These findings are consistent with a study by Jiang et al., which demonstrated the cytoprotective effect of alginate oligosaccharides on endothelial cells under oxidative stress, suggesting their potential antioxidant and antiapoptotic roles (Jiang et al., 2021). Similarly, the cytotoxic effect of Ibuprofen was evaluated against HUVEC cells to validate the assay. A dose of 100 μg/mL ibuprofen demonstrated its toxic potential, reducing cell viability to 44.22% after 24 hours of exposure. This inhibitory effect remained consistent at the 48-hour mark, with cell viability at 46.82%, confirming the cytotoxic nature of the compound at the tested concentration (Eldeeb et al., 2025; Habib et al., 2024) and its metabolites significantly influence the tumor development, and metastatic processes. The design and synthesis of prodrugs intended for nonsteroidal anti-inflammatory drugs (NSAIDs).

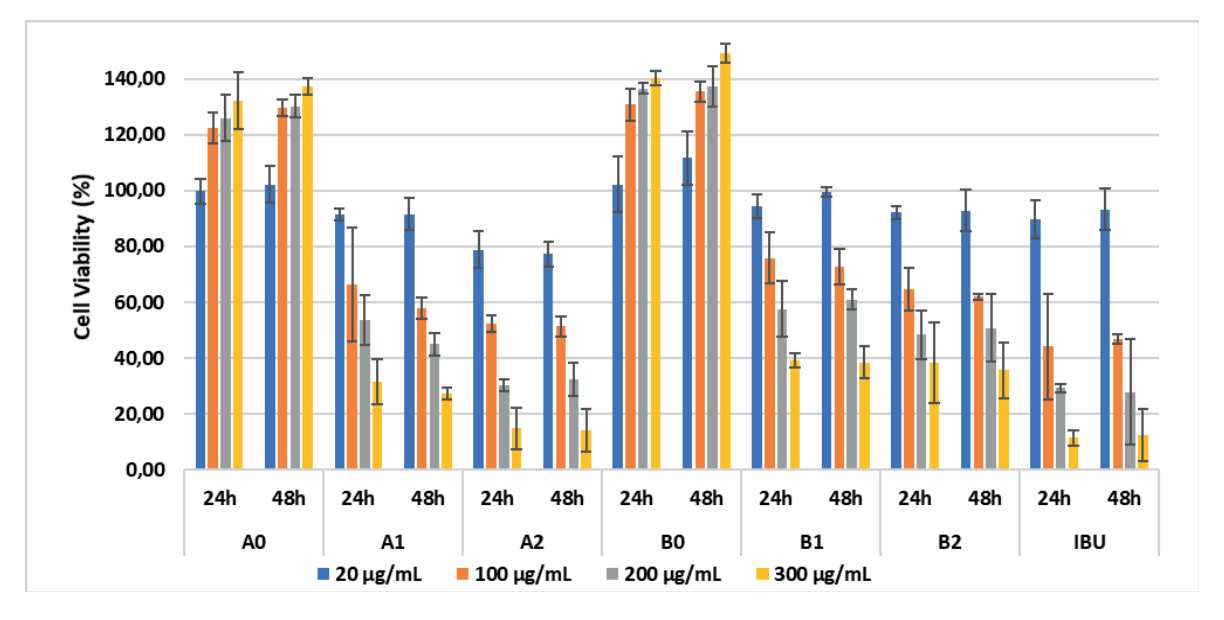


**Figure 5.** Cytotoxicity results (n = 3; mean  $\pm$  SD)

Formulations with a lower drug loading capacity were more effective at mitigating the active ingredient's cytotoxicity. This was particularly evident with Formulation B, which contained a higher alginate concentration and provided better protection than Formulation A. An example is the performance of Formulation B1, which maintained cell viability at 75.85% after 24 hours at 100 µg/mL, in contrast to Formulation A1, which resulted in a lower viability of 66.35%. Similar trends were observed in formulations with identical polymer composition but different loading capacities. At a concentration of 100 µg/mL for 24 hours, the lower loading capacity Formulation A1 showed 66.35% cell viability, while Formulation A2 resulted in a lower viability of 52.31%. Our findings suggest a correlation between the total amount of formulation and its ability to inhibit cytotoxicity, a result consistent with literature on other biocompatible polymers. Harrish et al. showed that chitosan, a natural and biodegradable polysaccharide similar to alginate, significantly reduced the toxicity of cadmium sulfide nanoparticles. This observation further highlights the potential of such polymers to improve the safety profile of active compounds and their formulations (Harish et al., 2020).

In conclusion, while the empty formulations were not found to be dose-dependently cytotoxic, the results of the MTT assays demonstrated that ibuprofen exhibited dose-dependent cytotoxicity. Importantly, the study revealed that the prepared formulations effectively mitigated this cytotoxic effect, highlighting the potential of the formulation design to enhance the safety profile of the active ingredient.

#### **CONCLUSION**

This study successfully prepared ibuprofen-loaded sodium alginate sponges with properties suitable for wound dressings. The sponges showed high swelling capacity and rapid dissolution. FTIR analysis confirmed molecular interactions that led to a significant

increase in the ibuprofen dissolution rate. The formulations also exhibited different drug release kinetics than pure ibuprofen, with some following the first-order and others the Hopfenberg models. Notably, the sponges were found to reduce the cytotoxicity of pure ibuprofen, highlighting their potential for further *in vivo* investigation as wound dressing applications.

#### **ACKNOWLEDGEMENTS**

We thank, Anadolu University Faculty of Pharmacy (MERLAB) for FTIR analyses and AUBİBAM for SEM analyses.

## **AUTHOR CONTRIBUTION STATEMENT**

KA: Concept, Design, Supervision, Manuscript Writing, Literature Search, Data Collection and Processing CKÖ: Literature Search, Data Collection, and Processing.

#### CONFLICT OF INTEREST

The authors declare that there is no conflict of interest.

#### REFERENCES

Anderson, K., & Hamm, R. L. (2012). Factors That Impair Wound Healing. *Journal of the American College of Clinical Wound Specialists*, 4(4), 84–91. https://doi.org/10.1016/j.jccw.2014.03.001

Andrgie, A. T., Darge, H. F., Mekonnen, T. W., Birhan, Y. S., Hanurry, E. Y., Chou, H. Y.,...Chang, Y. H. (2020a). Ibuprofen-Loaded Heparin Modified Thermosensitive Hydrogel for Inhibiting Excessive Inflammation and Promoting Wound Healing. *Polymers*, *12*(11), 2619. https://doi.org/10.3390/polym12112619

Andrgie, A. T., Darge, H. F., Mekonnen, T. W., Birhan, Y. S., Hanurry, E. Y., Chou, H. Y.,... Chang, Y. H. (2020b). Ibuprofen-Loaded Heparin Modified Thermosensitive Hydrogel for Inhibiting Excessive Inflammation and Promoting Wound Healing. *Polymers*, 12(11), 2619. https://doi.org/10.3390/polym12112619

- Arica, B., Çaliş, S., Atilla, P., Durlu, N. T., Çakar, N., Kaş, H. S., & Hincal, A. A. (2005). In vitro and in vivo studies of ibuprofen-loaded biodegradable alginate beads. *Journal of Microencapsulation*, 22(2), 153– 165. https://doi.org/10.1080/02652040400026319
- Askarizadeh, M., Esfandiari, N., Honarvar, B., Sajadian, S. A., & Azdarpour, A. (2023). Kinetic Modeling to Explain the Release of Medicine from Drug Delivery Systems. *ChemBioEng Reviews*, *10*(6), 1006–1049. https://doi.org/10.1002/cben.202300027
- Barbu, A., Neamtu, B., Zăhan, M., Iancu, G. M., Bacila, C., & Mireşan, V. (2021). Current Trends in Advanced Alginate-Based Wound Dressings for Chronic Wounds. *Journal of Personalized Medicine*, 11(9), 890. https://doi.org/10.3390/jpm11090890
- Boateng, J. S., Auffret, A. D., Matthews, K. H., Humphrey, M. J., Stevens, H. N. E., & Eccleston, G. M. (2010). Characterisation of freeze-dried wafers and solvent evaporated films as potential drug delivery systems to mucosal surfaces. *International Journal of Pharmaceutics*, 389(1), 24–31. https://doi.org/10.1016/j.ijpharm.2010.01.008
- Cañedo-Dorantes, L., & Cañedo-Ayala, M. (2019). Skin Acute Wound Healing: A Comprehensive Review. International Journal of Inflammation, 2019(1), 3706315. https://doi.org/10.1155/2019/3706315
- Chen, M. R., & Dragoo, J. L. (2013). The effect of nonsteroidal anti-inflammatory drugs on tissue healing. *Knee Surgery, Sports Traumatology, Arthroscopy*, 21(3), 540–549. https://doi.org/10.1007/ s00167-012-2095-2
- Chiaoprakobkij, N., Sanchavanakit, N., Subbalekha, K., Pavasant, P., & Phisalaphong, M. (2011). Characterization and biocompatibility of bacterial cellulose/alginate composite sponges with human keratinocytes and gingival fibroblasts. *Carbohydrate Polymers*, 85(3), 548–553. https://doi.org/10.1016/j.carbpol.2011.03.011
- Costa, P., & Sousa Lobo, J. M. (2001). Modeling and comparison of dissolution profiles. *European Journal of Pharmaceutical Sciences*, *13*(2), 123–133. https://doi.org/10.1016/S0928-0987(01)00095-1

- da Silva, C. M., Reis, R. L., Correlo, V. M., & Jahno, V. D. (2024). The efficient role of sodium alginate-based biodegradable dressings for skin wound healing application: A systematic review. *Journal of Biomaterials Science, Polymer Edition*, 35(3), 397–414. https://doi.org/10.1080/0920506 3.2023.2289247
- Dai, M., Zheng, X., Xu, X., Kong, X., Li, X., Guo, G.,...Qian, Z. (2009). Chitosan-Alginate Sponge: Preparation and Application in Curcumin Delivery for Dermal Wound Healing in Rat. *BioMed Research International*, 2009(1), 595126. https://doi.org/10.1155/2009/595126
- Djekic, L., Martinović, M., Ćirić, A., & Fraj, J. (2020). Composite chitosan hydrogels as advanced wound dressings with sustained ibuprofen release and suitable application characteristics. *Pharmaceuti*cal Development and Technology, 25(3), 332–339. https://doi.org/10.1080/10837450.2019.1701495
- Dokoumetzidis, A., & Macheras, P. (2006). A century of dissolution research: From Noyes and Whitney to the Biopharmaceutics Classification System. *International Journal of Pharmaceutics*, 321(1), 1–11. https://doi.org/10.1016/j.ijpharm.2006.07.011
- Eldeeb, A. M., Serag, E., Elmowafy, M., & El-Khouly, M. E. (2025). pH-responsive zeolite-A/chitosan nanocarrier for enhanced ibuprofen drug delivery in gastrointestinal systems. *International Journal of Biological Macromolecules*, 289, 138879. https://doi.org/10.1016/j.ijbiomac.2024.138879
- Farmer, S., Anderson, P., Burns, P., & Velagaleti, R. (2002). Forced Degradation of Ibuprofen in Bulk Drug and Tablets. *Pharmaceutical Technology*, 32, 28-42.
- Garzón, L. C., & Martínez, F. (2004). Temperature Dependence of Solubility for Ibuprofen in Some Organic and Aqueous Solvents. *Journal of Solution Chemistry*, 33(11), 1379–1395. https://doi. org/10.1007/s10953-004-1051-2
- Guo, S., & DiPietro, L. A. (2010). Factors Affecting Wound Healing. *Journal of Dental Research*, 89(3), 219–229. https://doi.org/10.1177/0022034509359125

- Gupta, A., Bhasarkar, J., Chandan, M. R., Shaik, A. H., Kiran, B., & Bal, D. K. (2020). Diffusion Kinetics of Vitamin B12 from Alginate and Poly(vinyl acetate) Based Gel Scaffolds for Targeted Drug Delivery. *Journal of Macromolecular Science, Part B*, 59(11), 713–730. https://doi.org/10.1080/0022234 8.2020.1800246
- Habib, S. M., Imran, M., Mansoor, F., Siddiqui, N. N., Jabeen, A., Jahan, H.,...Shah, M. R. (2024). Surface-modified nanoparticles based on ibuprofen prodrug and exploring its anti-inflammatory and anti-cancer potential. *Journal of Drug Delivery Science and Technology*, 100, 106021. https://doi.org/10.1016/j.jddst.2024.106021
- Harish, R., Nisha, K. D., Prabakaran, S., Sridevi, B., Harish, S., Navaneethan, M.,...Ganesh, M. R. (2020). Cytotoxicity assessment of chitosan coated CdS nanoparticles for bio-imaging applications. *Applied Surface Science*, 499, 143817. https://doi. org/10.1016/j.apsusc.2019.143817
- Higton, F. (2015). The Pharmaceutics of Ibuprofen. In *Ibuprofen* (pp. 51–80). John Wiley & Sons, Ltd. https://doi.org/10.1002/9781118743614.ch3
- Hu, S., Bi, S., Yan, D., Zhou, Z., Sun, G., Cheng, X., & Chen, X. (2018). Preparation of composite hydroxybutyl chitosan sponge and its role in promoting wound healing. *Carbohydrate Polymers*, 184, 154–163. https://doi.org/10.1016/j.carbpol.2017.12.033
- Huang, H., Grün, I. U., Ellersieck, M., & Clarke, A. D. (2017). Measurement of Total Sodium Alginate in Restructured Fish Products Using Fourier Transform Infrared Spectroscopy. EC Nutrion, 11(1), 33–45.
- Jan-Roblero, J., & Cruz-Maya, J. A. (2023). Ibuprofen: Toxicology and Biodegradation of an Emerging Contaminant. *Molecules*, 28(5), 2097. https://doi. org/10.3390/molecules28052097
- Janus, E., Ossowicz, P., Klebeko, J., Nowak, A., Duchnik, W., Kucharski, Ł., & Klimowicz, A. (2020). Enhancement of ibuprofen solubility and skin permeation by conjugation with 1 -valine alkyl esters. *RSC Advances*, 10(13), 7570–7584. https://doi.org/10.1039/D0RA00100G

- Jiang, Z., Zhang, X., Wu, L., Li, H., Chen, Y., Li, L.,... Zhu, Y. (2021). Exolytic products of alginate by the immobilized alginate lyase confer antioxidant and antiapoptotic bioactivities in human umbilical vein endothelial cells. *Carbohydrate Polymers*, 251, 116976. https://doi.org/10.1016/j.carbpol.2020.116976
- Kamari, Y., & Ghiaci, M. (2016). Preparation and characterization of ibuprofen/modified chitosan/ TiO2 hybrid composite as a controlled drug-delivery system. *Microporous and Mesoporous Materials*, 234, 361–369. https://doi.org/10.1016/j. micromeso.2016.07.030
- Katzhendler, I., Hoffman, A., Goldberger, A., & Friedman, M. (1997). Modeling of Drug Release from Erodible Tablets. *Journal of Pharmaceutical Sciences*, 86(1), 110–115. https://doi.org/10.1021/js9600538
- Kaynak, M. S., Soyseven, M., Kaval, B., Çelebier, M., Aygeyik, E., Şahin, S., & Arli, G. (2024). Exploring the correlation between ibuprofen solubility and permeability in intestinal disease conditions. ACTA Pharmaceutica Sciencia, 62(3), 593. https:// doi.org/10.23893/1307-2080.APS6238
- Khalil, R. M., Shalaby, E. S., Abdelhameed, M. F., Shabana, M. E.-A., & Wagdi, M. A. (2025). Novel surfactant-based elastic vesicular system as a promising approach for the topical delivery of Ibuprofen for enhanced wound healing. *Journal of Pharmaceutical Sciences*, 114(7), 103796. https:// doi.org/10.1016/j.xphs.2025.103796
- Khoukhi, O. E., Bahri, Z. E., Diaf, K., & Baitiche, M. (2016). Piroxicam /β-cyclodextrin complex included in cellulose derivatives-based matrix microspheres as new solid dispersion-controlled release formulations. *Chemical Papers*, 70(6), 828–839. https://doi.org/10.1515/chempap-2016-0014
- Kumar, S., Bhanjana, G., Sharma, A., Sidhu, M. C., & Dilbaghi, N. (2014). Synthesis, characterization and on field evaluation of pesticide loaded sodium alginate nanoparticles. *Carbohydrate Polymers*, 101, 1061–1067. https://doi.org/10.1016/j.carbpol.2013.10.025

- Latifah, R. N., Rahmania, S., & Rohmah, B. L. (2022). The effect of extraction time on the quality of brown seaweed Na-Alginate Sargassum polycisteum as the base material for SBK Edible Film. *Journal of Physics: Conference Series*, 2190(1), 012001. https://doi.org/10.1088/1742-6596/2190/1/012001
- Lawrie, G., Keen, I., Drew, B., Chandler-Temple, A., Rintoul, L., Fredericks, P., & Grøndahl, L. (2007). Interactions between Alginate and Chitosan Biopolymers Characterized Using FTIR and XPS. *Biomacromolecules*, 8(8), 2533–2541. https://doi. org/10.1021/bm070014y
- Li, Y., Fan, R., Xing, H., Fei, Y., Cheng, J., & Lu, L. (2021). Study on swelling and drug releasing behaviors of ibuprofen-loaded bimetallic alginate aerogel beads with pH-responsive performance. *Colloids and Surfaces B: Biointerfaces*, 205, 111895. https://doi.org/10.1016/j.colsurfb.2021.111895
- Li, Y., & Yang, L. (2015). Driving forces for drug loading in drug carriers. *Journal of Microencapsulation*, 32(3), 255–272. https://doi.org/10.3109/026 52048.2015.1010459
- Liu, J., Xiao, J., Li, F., Shi, Y., Li, D., & Huang, Q. (2018). Chitosan-sodium alginate nanoparticle as a delivery system for ε-polylysine: Preparation, characterization and antimicrobial activity. *Food Control*, 91, 302–310. https://doi.org/10.1016/j. foodcont.2018.04.020
- Liu, Q., Jing, Y., Han, C., Zhang, H., & Tian, Y. (2019). Encapsulation of curcumin in zein/ caseinate/ sodium alginate nanoparticles with improved physicochemical and controlled release properties. *Food Hydrocolloids*, 93, 432–442. https://doi.org/10.1016/j.foodhyd.2019.02.003
- Long, L., Liu, W., Hu, C., Yang, L., & Wang, Y. (2022). Construction of multifunctional wound dressings with their application in chronic wound treatment. *Biomaterials Science*, *10*(15), 4058–4076. https://doi.org/10.1039/D2BM00620K
- Lv, C., Zhou, X., Wang, P., Li, J., Wu, Z., Jiao, Z.,... Zhang, P. (2022). Biodegradable alginate-based sponge with antibacterial and shape memory properties for penetrating wound hemostasis. *Composites Part B: Engineering*, 247, 110263. https://doi.org/10.1016/j.compositesb.2022.110263

- Majid Khan, G., & Bi Zhu, J. (1998). Ibuprofen release kinetics from controlled-release tablets granulated with aqueous polymeric dispersion of ethylcellulose II: Influence of several parameters and coexcipients. *Journal of Controlled Release*, 56(1), 127–134. https://doi.org/10.1016/S0168-3659(98)00080-7
- Martín-Illana, A., Cazorla-Luna, R., Notario-Pérez, F., Rubio, J., Ruiz-Caro, R., Tamayo, A., & Veiga, M. D. (2022). Eudragit\* L100/chitosan composite thin bilayer films for intravaginal pH-responsive release of Tenofovir. *International Journal of Pharmaceutics*, 616, 121554. https://doi.org/10.1016/j.ijpharm.2022.121554
- Mohandas, A., Nimal, T. R., Das, V., Shankarappa, S. A., Biswas, R., & Jayakumar, R. (2015). Drug loaded bi-layered sponge for wound management in hyperfibrinolytic conditions. *Journal of Materials Chemistry B*, *3*(28), 5795–5805. https://doi.org/10.1039/C5TB00568J
- Mohiti-Asli, M., Saha, S., Murphy, S. v., Gracz, H., Pourdeyhimi, B., Atala, A., & Loboa, E. G. (2017). Ibuprofen loaded PLA nanofibrous scaffolds increase proliferation of human skin cells in vitro and promote healing of full thickness incision wounds in vivo. *Journal of Biomedical Materials Research Part B: Applied Biomaterials*, 105(2), 327–339. https://doi.org/10.1002/jbm.b.33520
- Morgado, P. I., Miguel, S. P., Correia, I. J., & Aguiar-Ricardo, A. (2017). Ibuprofen loaded PVA/chitosan membranes: A highly efficient strategy towards an improved skin wound healing. *Carbohydrate Polymers*, 159, 136–145. https://doi.org/10.1016/j.carbpol.2016.12.029
- Muselík, J., Komersová, A., Kubová, K., Matzick, K., & Skalická, B. (2021). A Critical Overview of FDA and EMA Statistical Methods to Compare In Vitro Drug Dissolution Profiles of Pharmaceutical Products. *Pharmaceutics*, 13(10), 1703. https:// doi.org/10.3390/pharmaceutics13101703

- Naghshineh, N., Tahvildari, K., & Nozari, M. (2019). Preparation of Chitosan, Sodium Alginate, Gelatin and Collagen Biodegradable Sponge Composites and their Application in Wound Healing and Curcumin Delivery. *Journal of Polymers and the Environment*, 27(12), 2819–2830. https://doi.org/10.1007/s10924-019-01559-z
- Namazi, Z., Jafarzadeh Kashi, T. S., Erfan, M., Najafi, F., Bakhtiari, L., Ghodsi, S. R., & Farhadnejad, H. (2019). Facile Synthesis and Characterization of Ibuprofen-mesoporous Hydroxyapatite Nanohybrid as a Sustained Drug Delivery System. *Iranian Journal of Pharmaceutical Research*: *IJPR*, 18(3), 1196–1211. https://doi.org/10.22037/ ijpr.2019.1100769
- Namazov, K. (2022). İBUPROFEN YÜKLÜ POLİM-ERİK NANOPARTİKÜLLERİN HAZIRLAN-MASI VE İN VİTRO DEĞERLENDİRİLMESİ [Master's thesis, Anadolu Üniversitesi]. Retrieved from [chrome-extension://efaidnbmnnnibpcajpcglclefindmkaj/https://core.ac.uk/download/643454459.pdf]
- Paarakh, M. P., Jose, P. A., Setty, C., & Peterchristoper, G. V. (2018). RELEASE KINETICS CONCEPTS AND APPLICATIONS. *International Journal of Pharmacy Research & Technology (IJPRT)*, 8(1), 12–20. https://doi.org/10.31838/ijprt/08.01.02
- Pazyar, N., Yaghoobi, R., Rafiee, E., Mehrabian, A., & Feily, A. (2014). Skin Wound Healing and Phytomedicine: A Review. *Skin Pharmacology and Physiology*, *27*(6), 303–310. https://doi.org/10.1159/000357477
- Peña, O. A., & Martin, P. (2024). Cellular and molecular mechanisms of skin wound healing. *Nature Reviews Molecular Cell Biology*, 25(8), 599–616. https://doi.org/10.1038/s41580-024-00715-1
- Petchsomrit, A., Sermkaew, N., & Wiwattanapatapee, R. (2017). Alginate-Based Composite Sponges as Gastroretentive Carriers for Curcumin-Loaded Self-Microemulsifying Drug Delivery Systems. *Scientia Pharmaceutica*, 85(1), 11. https://doi.org/10.3390/scipharm85010011

- Price, P., Fogh, K., Glynn, C., Krasner, D. L., Osterbrink, J., & Sibbald, R. G. (2007). Why combine a foam dressing with ibuprofen for wound pain and moist wound healing? *International Wound Journal*, 4(s1), 1–3. https://doi.org/10.1111/j.1742-481X.2007.00310.x
- Priese, F., Wiegel, D., Funaro, C., Mondelli, G., & Wolf, B. (2023). Comparison of Mini-Tablets and Pellets as Multiparticulate Drug Delivery Systems for Controlled Drug Release. *Coatings*, *13*(11), 1891. https://doi.org/10.3390/coatings13111891
- Rainsford, K. D. (2009). Ibuprofen: Pharmacology, efficacy and safety. *Inflammopharmacology*, *17*(6), 275–342. https://doi.org/10.1007/s10787-009-0016-x
- Ramukutty, S., & Ramachandran, E. (2012). Growth, spectral and thermal studies of ibuprofen crystals. *Crystal Research and Technology*, *47*(1), 31–38. https://doi.org/10.1002/crat.201100394
- Romanelli, M., Dini, V., Polignano, R., Bonadeo, P., & Maggio, G. (2009). Ibuprofen slow-release foam dressing reduces wound pain in painful exuding wounds: Preliminary findings from an international real-life study. *Journal of Dermatological Treatment*, 20(1), 19–26. https://doi.org/10.1080/09546630802178232
- Romani, C., Sponchioni, M., & Volonterio, A. (2024). Fluorinated PAMAM-Arginine Carrier Prodrugs for pH-Sensitive Sustained Ibuprofen Delivery. *Pharmaceutical Research*, 41(8), 1725–1736. https://doi.org/10.1007/s11095-024-03747-6
- Sadeghi-Aghbash, M., Rahimnejad, M., Adeli, H., & Feizi, F. (2023). Wound Healing: An Overview of Wound Dressings on Health Care. *Current Pharmaceutical Biotechnology*, 24(9), 1079–1093. https://doi.org/10.2174/138920102366622091315 3725
- Schultz, G. S., Chin, G. A., Moldawer, L., & Diegelmann, R. F. (2011). Principles of Wound Healing. In R. Fitridge & M. Thompson (Eds.), *Mechanisms of Vascular Disease: A Reference Book for Vascular Specialists*. University of Adelaide Press. http://www.ncbi.nlm.nih.gov/books/NBK534261/

- Shaikh, M. A. J., Alharbi, K. S., Almalki, W. H., Imam, S. S., Albratty, M., Meraya, A. M.,...Gupta, G. (2022). Sodium alginate based drug delivery in management of breast cancer. *Carbohydrate Polymers*, 292, 119689. https://doi.org/10.1016/j.carbpol.2022.119689
- Sorg, H., Tilkorn, D. J., Hager, S., Hauser, J., & Mirastschijski, U. (2017). Skin Wound Healing: An Update on the Current Knowledge and Concepts. *European Surgical Research*, *58*(1–2), 81–94. https://doi.org/10.1159/000454919
- Stoyanova, K., Vinarov, Z., & Tcholakova, S. (2016). Improving Ibuprofen solubility by surfactant-facilitated self-assembly into mixed micelles. *Journal of Drug Delivery Science and Technology*, *36*, 208–215. https://doi.org/10.1016/j.jddst.2016.10.011
- Tenorová, K., Masteiková, R., Pavloková, S., Kostelanská, K., Bernatonienė, J., & Vetchý, D. (2022). Formulation and Evaluation of Novel Film Wound Dressing Based on Collagen/Microfibrillated Carboxymethylcellulose Blend. *Pharmaceutics*, *14*(4), 782. https://doi.org/10.3390/pharmaceutics14040782
- Tottoli, E. M., Dorati, R., Genta, I., Chiesa, E., Pisani, S., & Conti, B. (2020). Skin Wound Healing Process and New Emerging Technologies for Skin Wound Care and Regeneration. *Pharmaceutics*, 12(8), 735. https://doi.org/10.3390/pharmaceutics12080735
- Üstünes, L. (2025). *RxMediaPharma*\* (Version 2025) [Computer software]. GEMAŞ Genel Mühendislik Mekanik Sanayi ve Ticaret A.Ş.
- Velnar, T., Bailey, T., & Smrkolj, V. (2009). The Wound Healing Process: An Overview of the Cellular and Molecular Mechanisms. *Journal of International Medical Research*, *37*(5), 1528–1542. https://doi.org/10.1177/147323000903700531
- Vidart, J. M. M., Silva, T. L. da, Rosa, P. C. P., Vieira, M. G. A., & Silva, M. G. C. da. (2018). Development of sericin/alginate particles by ionic gelation technique for the controlled release of diclofenac sodium. *Journal of Applied Polymer Science*, 135(12), 45919. https://doi.org/10.1002/app.45919

- Wang, D., Sun, Y., Zhang, D., Kong, X., Wang, S., Lu, J.,...Zhou, Q. (2023). Root-shaped antibacterial alginate sponges with enhanced hemostasis and osteogenesis for the prevention of dry socket. *Carbohydrate Polymers*, 299, 120184. https://doi.org/10.1016/j.carbpol.2022.120184
- Wang, Y., Lu, H., Guo, M., Chu, J., Gao, B., & He, B. (2022). Personalized and Programmable Microneedle Dressing for Promoting Wound Healing. Advanced Healthcare Materials, 11(2), 2101659. https://doi.org/10.1002/adhm.202101659
- Xie, Y., Gao, P., He, F., & Zhang, C. (2022). Application of Alginate-Based Hydrogels in Hemostasis. *Gels*, 8(2), 109. https://doi.org/10.3390/gels8020109
- Yalçınkaya, K., Senel, B., & Akyıl, E. (2025). Formulation, Characterization and Cytotoxic Effect of Indomethacin-loaded Nanoparticles. Anti-Inflammatory & Anti-Allergy Agents in Medicinal Chemistry, 24(2), 139–148. https://doi.org/10.2174/0118715230348349241126053733
- Yang, F., Bai, X., Dai, X., & Li, Y. (2021). The Biological Processes During Wound Healing. Regenerative Medicine, 16(4), 373–390. https://doi.org/10.2217/ rme-2020-0066
- Yurtdaş-Kırımlıoğlu, G., Özer, S., Büyükköroğlu, G., & Yazan, Y. (2018). Formulation and In Vitro Evaluation of Moxifloxacin Hydrochloride-Loaded Polymeric Nanoparticles for Ocular Application. *Latin American Journal of Pharmacy*, 37(9), 1850-1862
- Zhang, Y., Huo, M., Zhou, J., Zou, A., Li, W., Yao, C., & Xie, S. (2010). DDSolver: An Add-In Program for Modeling and Comparison of Drug Dissolution Profiles. *The AAPS Journal*, *12*(3), 263–271. https://doi.org/10.1208/s12248-010-9185-1
- Zhang, Z., Liu, H., Yu, D. G., & Bligh, S. W. A. (2024).
  Alginate-Based Electrospun Nanofibers and the Enabled Drug Controlled Release Profiles:
  A Review. *Biomolecules*, 14(7), 789. https://doi.org/10.3390/biom14070789
- Zuo, J., Gao, Y., Bou-Chacra, N., & Löbenberg, R. (2014). Evaluation of the DDSolver Software Applications. *BioMed Research International*, 2014(1), 204925. https://doi.org/10.1155/2014/204925